Thermochimica Acta, 65 (1983) 197–212
Elsevier Science Publishers B.V., Amsterdam – Printed in The Netherlands

THERMAL ANALYSIS OF ANTIMONY/POTASSIUM PERMANGANATE PYROTECHNIC COMPOSITIONS

MICHAEL W. BECK and MICHAEL E. BROWN *

Chemistry Department, Rhodes University, Grahamstown 6140 (South Africa)

(Received 10 December 1982)

ABSTRACT

Results of a detailed thermoanalytical study of the $Sb/KMnO_4$ pyrotechnic system, including the reactions of the individual constituents in air, are reported. The ignition reaction occurs under certain conditions of thermal analysis, the most important of which is that there should be oxygen available in the carrrier gas used. In sealed delay elements, oxygen is supplied by the first stage of the decomposition of $KMnO_4$, which takes place at relatively low temperatures (~ 300°C).

The ignition reaction is observed in the temperature range (~ 500°C) over which Sb powder, alone, is fairly rapidly oxidised on heating in air. The presence of Mn, either as the metal powder physically mixed with Sb, or as the intermetallic compound MnSb, affects the course of the Sb oxidation and this effect extends to the presence of MnO_2, K_2MnO_4 and the products of decomposition of $KMnO_4$. There is an interaction between Sb and these compounds when heated in nitrogen, but this does not lead to ignition, and the product in nitrogen, when reheated in air, does not ignite.

Results of attempts to identify the reactions occurring using X-ray diffraction, infrared spectroscopy, and optical and electron microscopy are described.

INTRODUCTION

Considerable success in determining the mechanisms of intersolid pyrotechnic reactions has been achieved through use of thermal analysis [1]. It does not necessarily follow, of course, that the reactions taking place under the generally more-controlled conditions of thermal analysis are identical to those occurring when the pyrotechnic compositions are ignited. The conditions used for thermal analysis may allow the occurrence of phase changes and slow reactions, as well as the escape of evolved gases, which do not have time to occur when ignition is by fuse [2]. Thermal analysis does, however, provide a starting point for the unravelling of the complex processes involved, and can produce useful thermochemical, and in favourable cases,

* To whom correspondence should be addressed.

0040-6031/83/$03.00

kinetic information [3]. Results obtained may then be combined with results from techniques such as temperature profile analysis [4] to construct a complete picture of the ignition process. Attempts have been made to link these two approaches more closely through use of high heating-rate thermal analysis [2] of very small samples.

In this paper, results of a detailed thermoanalytical study of the reactions in the antimony/potassium permanganate system, which has been in use for many years as a delay composition, are presented. Starting points for such a study were the reports on the thermal decomposition of potassium permanganate [5,6], and the references therein, and thermal analyses of the oxides of antimony [7]. Some thermal analyses on the antimony/potassium permanganate system have also been reported by Nakahara [8], who has also studied the pressure and temperature rises during the ignition process [9].

EXPERIMENTAL

The equipment used included a Perkin-Elmer DSC-2 differential scanning calorimeter, a Stanton Redcroft STA 781 simultaneous DTA/TG system and a Stanton Redcroft hot-stage microscope. Reactions occurring above the 500°C limit for use of aluminium pans, were studied using gold pans, with lids, but without crimping, in the DSC, and platinum cups in the DTA/TG system.

Surface textures of the solid phases, before, after and at suitable stages of reaction, were examined using scanning electron microscopy. X-Ray diffraction (XRD) and infrared (IR) spectroscopy (of samples in KBr disks, with which $KMnO_4$ does not react [10]) were used in attempts to identify reaction intermediates and products.

Materials. The powdered potassium permanganate and antimony used were supplied by AECI Limited. The permanganate, and all other oxidants used were sieved through a 53 μm mesh before being mixed with the metal fuel. The average particle size of the Sb powder was considerably less ($\sim 1/5$ the diameter) than that of the $KMnO_4$ particles and had a specific surface area (BET) of 1.48 $m^2\ g^{-1}$. Mixing was accomplished by end-over-end tumbling in the presence of small rubber balls. The mixes were investigated in the loose powdered form and as pellets formed by compaction at a pressure of 200 kPa in a single-punch press.

Other oxidants used were potassium manganate (prepared according to Scholder and Waterstradt [11] and dried and stored under vacuum over P_2O_5), rubidium permanganate (prepared [12] from potassium permanganate and rubidium chloride), and commercially available (Merck) manganese dioxide (< 53 μm fraction, specific surface area 69.8 $m^2\ g^{-1}$).

Some runs were also done using alloys of antimony, NiSb and MnSb (Cerac, USA; < 150 μm) in combination with $KMnO_4$.

RESULTS AND DISCUSSION

Thermal decomposition of the oxidants

$KMnO_4$. The thermal behaviour of $KMnO_4$ in the temperature range 25–900°C in air and in nitrogen has been studied extensively [5,6]. Decomposition occurs in two discrete stages. DTA traces (Fig. 1) show a sharp exotherm at about 290°C and an endotherm at approximately 620°C. Simultaneous TG measurements show a rapid mass loss at 290°C of ~ 12.0% of the initial mass followed by a gradual mass loss until 620°C when the second stage (~ 3.5% of the original mass) is observed.

Herbstein et al. [5], from both thermal and chemical analyses, proposed that the stoichiometry of the first stage of decomposition is

$$10\ KMnO_{4(s)} \rightarrow 2.65\ K_2MnO_{4(s)} + (2.35\ K_2O \cdot 7.35\ MnO_{2.05})_{(s)} + 6\ O_{2(g)}$$

corresponding to a mass loss of 12.1% {Nakahara [8] and many other workers have proposed

$$2\ KMnO_{4(s)} \rightarrow K_2MnO_{4(s)} + MnO_{2(s)} + O_{2(g)}$$

corresponding to a mass loss of 10.1%, while Boldyrev et al. [13,14] have shown that $K_3(MnO_4)_{2(s)}$ is an intermediate in the formation of K_2MnO_4.}

The second stage was represented [5] as

$$10\ K_2MnO_{4(s)} \rightarrow 5.7\ K_3MnO_{4(s)} + 0.5(2.9\ K_2O \cdot 8.6\ MnO_{2.1})_{(s)} + 3.4\ O_{2(g)}$$

and was found to be reversible in air.

DSC scans were used to estimate the enthalpies of the decomposition stages. The values obtained were -69.1 ± 0.9 J g^{-1} or -10.9 ± 0.1 kJ (mole $KMnO_4)^{-1}$ for the exotherm (in agreement with -10.5 kJ $mole^{-1}$ reported

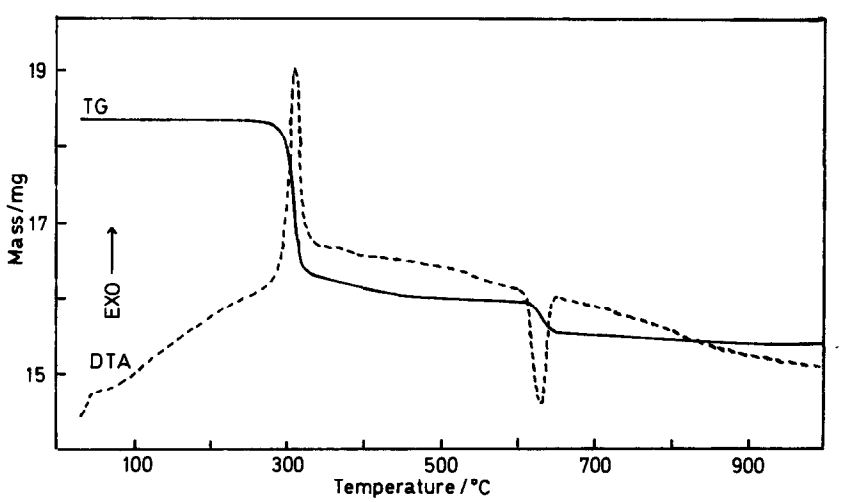

Fig. 1. Simultaneous TG/DTA on $KMnO_4$ powder in air at 20°C min^{-1}.

by Herbstein et al. [5]), and 102 ± 3 J g^{-1} or 16.1 ± 0.5 kJ (mole $KMnO_4$)$^{-1}$ for the endotherm.

$RbMnO_4$. Rubidium permanganate also decomposes in two stages, similar in form and temperature ranges to those for $KMnO_4$. Herbstein et al. [5] have reported on the detailed stoichiometry. Crystals of $RbMnO_4$ shatter in a similar way to $KMnO_4$ when heated on the hot-stage microscope, and no melting was observed. The shattering process can cause some irreproducibility in the DSC record of the first stage of the decomposition.

K_2MnO_4. A sample of potassium manganate, prepared from solution, on heating in air gave a single endotherm at ~ 640°C (Fig. 2). On cooling to room temperature and reheating, the endotherm was again evident indicating at least partial reversibility of the decomposition. The value of ΔH for the original scan was 282 ± 8 J g^{-1} (decreasing to ~ 100 J g^{-1} on repetition). This value would correspond to that measured for the second stage of the $KMnO_4$ decomposition based on the stoichiometry of Herbstein et al. [5] and the assumption that only K_2MnO_4 decomposed in this stage.

The oxidation of antimony

Some thermal analysis work on the oxides of antimony has been reported [7]. Three stable oxides exist: Sb_2O_3 (in two forms, orthorhombic < 570°C, cubic > 570°C), Sb_2O_4 and Sb_2O_5. On heating Sb_2O_3 in air, oxidation to Sb_2O_4 occurs around 465°C. At these temperatures, considerable volatilisation of unreacted Sb_2O_3 can occur. Sb_2O_4 is stable in air or nitrogen up to 1000°C, dissociating above this temperature into Sb_2O_3 and oxygen. Sb_2O_5 starts losing oxygen above 400°C and by 900°C has formed stoichiometric Sb_2O_4.

Simultaneous TG/DTA traces obtained on heating antimony powder in air are shown in Fig. 3. The small exotherm at ~ 300°C corresponds to an

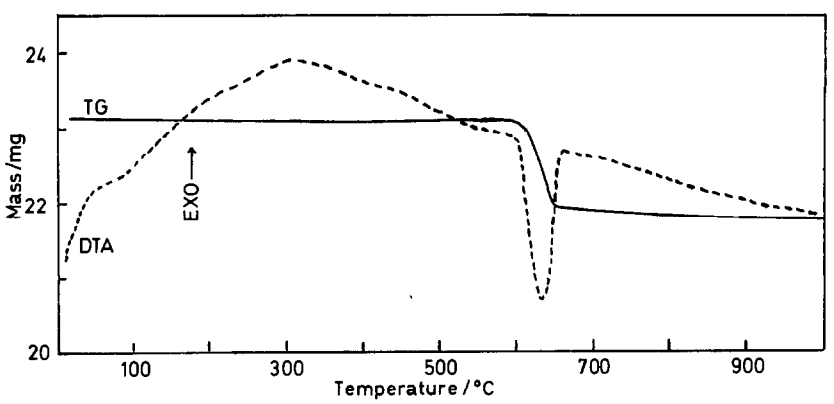

Fig. 2. Simultaneous TG/DTA on K_2MnO_4 powder in air at 20°C min^{-1}.

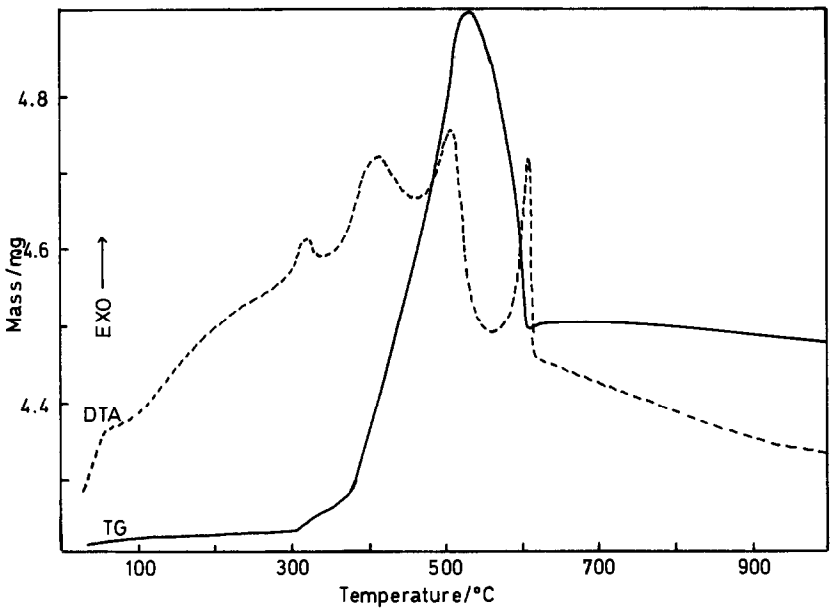

Fig. 3. Simultaneous TG/DTA on Sb powder in air at 20°C min^{-1}.

increase in mass of ~ 1%. The small amount of surface oxide formed at this stage, accompanied by visible darkening under the hot-stage microscope, was not distinguishable by XRD from the original antimony pattern with small traces of lead. A rapid, but not very reproducible, increase in mass of about $16 \pm 2\%$ occurs between 300 and 500°C, followed by a sharp mass loss and final formation of a stable product at ~ 600°C.

The probable oxidation steps, together with their expected mass increases (based on the original mass of antimony used) and expected standard enthalpies of reaction are

$$Sb_{(s)} + \tfrac{3}{4}\, O_{2(g)} \rightarrow \tfrac{1}{2}\, Sb_2O_{3(s)} \qquad (19.7\%) \qquad \Delta H^{\theta} = -348 \text{ kJ (mole Sb)}^{-1}$$

$$\tfrac{1}{2}\, Sb_2O_{3(s)} + \tfrac{1}{2}\, O_{2(g)} \rightarrow \tfrac{1}{2}\, Sb_2O_{4(s)} \qquad (6.5\%) \qquad \Delta H^{\theta} = -99.4 \text{ kJ (mole Sb)}^{-1}$$

The TG results of Nakahara [8] for oxidation of Sb in air, show an overall mass gain of ~ 25% in two approximately equal stages (230–300°C and 450–600°C).

The DTA trace (Fig. 3) and a DSC trace (Fig. 4a) show several overlapping exotherms. The total area under these exotherms corresponds to an enthalpy change of −330 kJ (mole Sb)$^{-1}$ which is lower than the overall standard value of −448 kJ (mole Sb)$^{-1}$ calculated for oxidation to the tetroxide. The valleys between exotherms are probably superimposed endothermic contributions from volatilisation and/or melting [15]. [Sb melts at 630.5°C with $\Delta H_{fusion} = 20.1$ kJ mole^{-1}; $Sb_2O_{3(s)}$ undergoes a cubic to

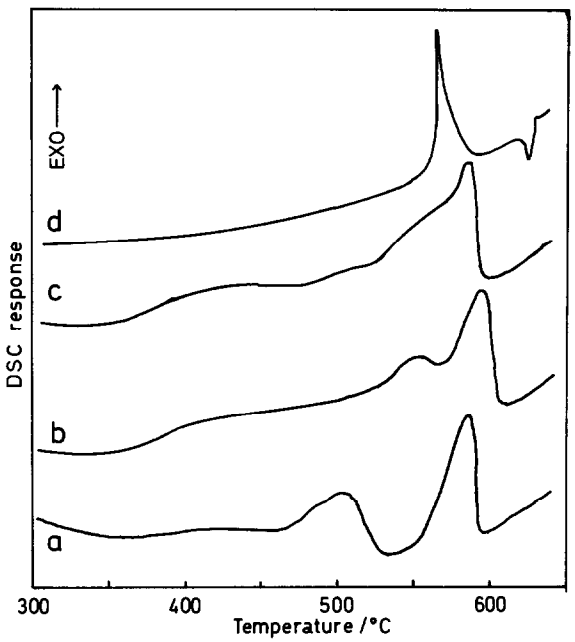

Fig. 4. DSC on (a) Sb; (b) 14.3% Mn/Sb; (c) 22.6% Mn/Sb; and (d) MnSb (31.1% Mn) in air at 20°C min^{-1}.

orthorhombic transition at 557°C with $\Delta H_{trans} = 3.4$ kJ (mole Sb)$^{-1}$, and then melts at 655°C with $\Delta H_{fusion} = 30.9$ kJ (mole Sb)$^{-1}$. The enthalpy of vaporisation of $Sb_2O_{3(l)}$ at 1456°C and 1 atm is 18.7 kJ (mole Sb)$^{-1}$, so that for $\frac{1}{2}$ $Sb_2O_{3(s)} \rightarrow \frac{1}{2}$ $Sb_2O_{3(g)}$, $\Delta H \simeq 50$ kJ (mole Sb)$^{-1}$.] Therefore, deviations from the expected mass changes and ΔH values, probably arise from the combined effects of the volatility of Sb_2O_3 and incomplete oxidation of some of the Sb. This is confirmed by the results of heating samples of Sb_2O_3 (Riedel-de-Haën) in air, when the exothermic step at ~ 530°C gave a mass increase of only 2.4% instead of the expected 5.5% of the original mass of Sb_2O_3. XRD confirmed the formation of cubic Sb_2O_3 (senarmontite) at ~ 530°C, and that the final product was Sb_2O_4.

In comparison to antimony itself, nickel antimonide, NiSb, was resistant to oxidation on heating in air over the accessible temperature range (< 720°C). Manganese antimonide, MnSb, however, undergoes a strongly exothermic reaction, characteristic of ignition, when heated in air above 550°C (Fig. 4d). Manganese powder, itself, is not oxidised below 720°C. The oxidation of mixtures of manganese and antimony powders is compared with the oxidation of Sb alone, and of MnSb, in Fig. 4. It is clear that the presence of Mn modifies the oxidation of Sb considerably even if originally present only as a physical mixture.

The Sb / $KMnO_4$ system

A composition of 60% Sb/40% $KMnO_4$ by mass was chosen as reference, as this composition lies on the plateau of the burning-rate curve, Fig. 5, where fairly large changes in composition do not change the burning characteristics and hence, presumably, do not significantly change the reactions occurring. Simultaneous TG/DTA curves for this composition in air are shown in Fig. 6. DSC and DTA results were similar and are comparable with results reported by Nakahara [8]. The small exotherm at ~ 300°C is associated with a mass loss of about 4.5%. This corresponds in position to the first stage of the decomposition of $KMnO_4$ on its own (Fig. 1), although this is also the temperature range at which some initial oxidation of Sb occurs (Fig. 3).

The exothermic shoulder at ~ 440°C (accompanied by a gradual mass gain) is followed by a strong, sharp exotherm at ~ 490°C (with an associated rapid increase in mass). This sharp exotherm is attributed to sample ignition. Pressing the sample into a small pellet had very little effect on the thermograms. The ignition exotherm is not observed when slow heating rates ($< 20°C\ min^{-1}$), small samples masses (< 1.5 mg), or very spread out samples are used.

The post-ignition exotherms at 580–600°C are accompanied by a further

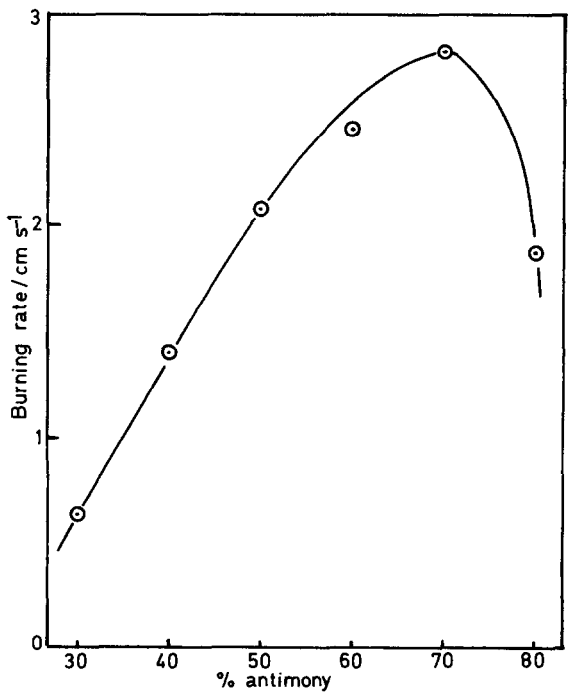

Fig. 5. Burning rates of Sb/$KMnO_4$ compositions.

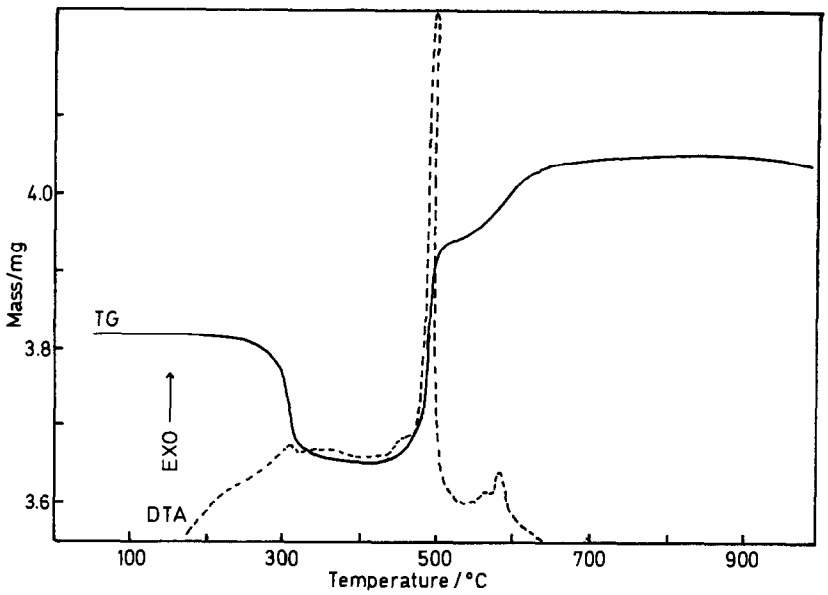

Fig. 6. Simultaneous TG/DTA on 60% Sb/$KMnO_4$ in air at 20°C min^{-1}.

gradual increase in sample mass, but could also include some contributions from solidification of molten material. Measurement of the total exothermicity gave a value of $\Delta H = -2.11 \pm 0.03$ kJ (g of mixture)$^{-1}$.

When heated in nitrogen, the 60% Sb/$KMnO_4$ mixture behaved as shown in Fig. 7. The exotherm and mass loss at ~ 300°C, attributable to the first stage of the decomposition of $KMnO_4$, are followed by a series of broad exotherms with no sharp ignition peak and no significant changes of mass.

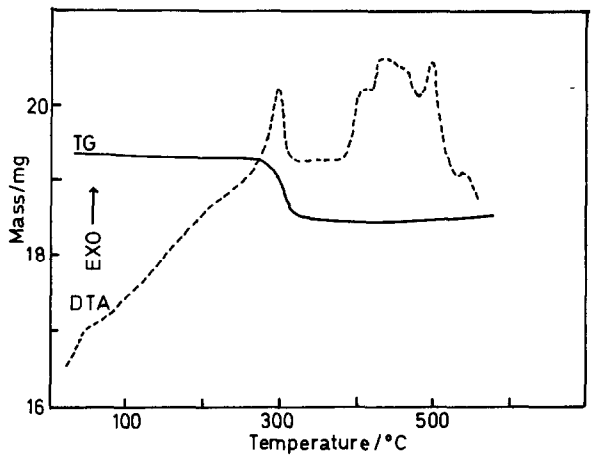

Fig. 7. Simultaneous TG/DTA on 60% Sb/$KMnO_4$ in nitrogen at 20°C min^{-1}. (Note increased sample mass.)

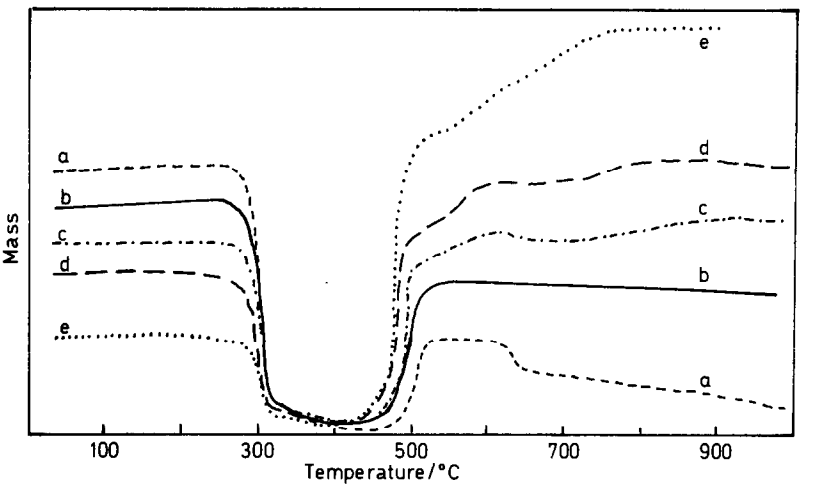

Fig. 8. TG responses for a range of $Sb/KMnO_4$ compositions in air at 20°C min^{-1}. Percentage Sb by mass (a) 20; (b) 30; (c) 40; (d) 50; (e) 70.

Partial melting was observed at ~ 540°C under the hot-stage microscope, so the DTA trace may be the resultant of some endothermic melting contributions superimposed on the exothermic oxidation. When the product of a scan to 520°C in nitrogen was rerun in air, the sharp ignition exotherm of Fig. 6 was replaced by broad overlapping exotherms with ΔH reduced to ~ 1.1 kJ g^{-1}.

The effect of varying the fuel / oxidant ratio

TG curves for a range of fuel/oxidant ratios (Fig. 8) show that the mass loss at ~ 300°C decreases with decreasing proportion of oxidant, as would

TABLE 1

Mass losses for the initial exothermic reaction of $Sb/KMnO_4$ mixes

% Sb	Mass losses	
	Expected (for $KMnO_4$ decomposition) (%)	Found (%)
20	9.6	9.4
30	8.4	8.6
40	7.2	6.7
50	6.0	5.8
60	4.8	4.3
70	3.6	3.3

TABLE 2

Mass changes calculated for the oxidation of Sb

% Fuel	Mass increase			
	based on Sb_2O_3 product (%)	based on Sb_2O_4 product (%)	including loss through $KMnO_4$ second stage (%)	Experimental (%)
20	3.9	5.2	3.0	3.3
30	5.9	7.9	6.0	5.3
40	7.9	10.5	8.9	7.6
50	9.9	13.2	11.8	8.9
60	11.8	15.8	14.7	12.5
70	13.8	18.4	17.6	14.8

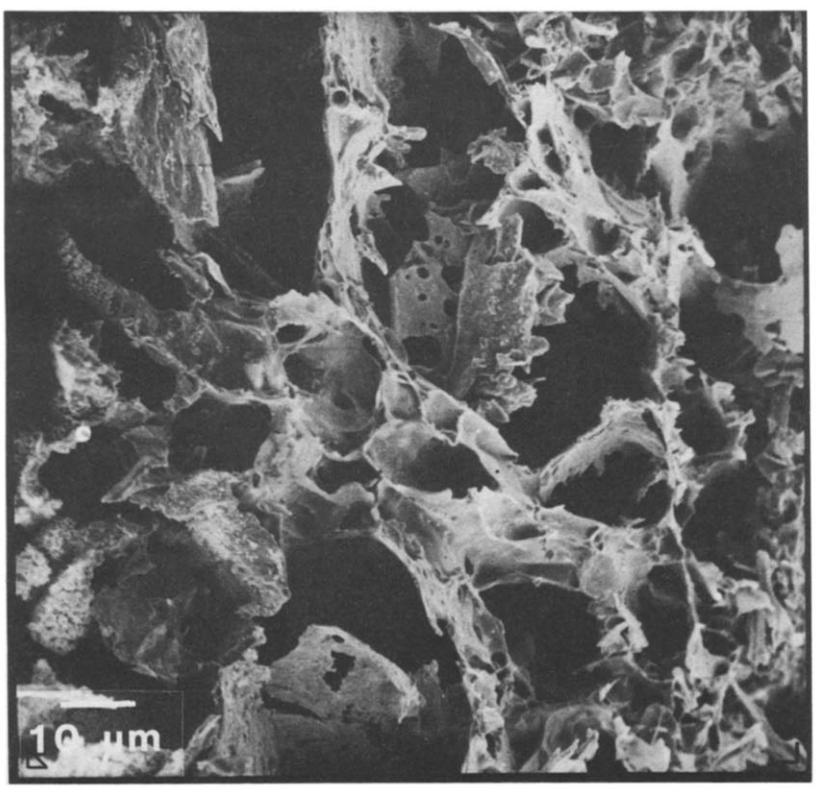

Fig. 9. Scanning electron micrograph of the product of ignition of a 60% Sb/$KMnO_4$ composition.

be expected for the first stage of the decomposition of $KMnO_4$ (Table 1), while the overall mass gain during the ignition exotherm increases. The amount of post-ignition reaction (580–600°C) also decreases with decreasing fuel content. This is probably normal oxidation in air of excess antimony, in the absence of the promoting effect of the $KMnO_4$ residue. The measured increases in mass fall short of those calculated for complete oxidation of Sb to Sb_2O_4 without loss of Sb_2O_3(Table 2).

The mass loss on decomposition of $KMnO_4$ is approximately balanced by the mass gain on oxidation for the 40% $Sb/KMnO_4$ composition. In sealed delay elements, mixes with fuel content lower than 40% would be unnecessarily gassy. Higher fuel contents would result in incomplete oxidation of the antimony.

The initial reaction of a 60% $Sb/KMnO_4$ mix at ~ 300°C can be seen, under the hot-stage microscope, to be accompanied by shattering of particles as observed for $KMnO_4$ at this temperature. No other processes are visible until ignition occurs at ~ 490°C. A bright, orange glow originates at a hot-spot in the sample and travels rapidly through the unreacted mixture. The reaction front has a molten appearance, especially for mixtures with high fuel ratios. The occurrence of some melting is confirmed by the foam-like appearance of scanning electron micrographs of the product of ignition in a delay element (Fig. 9). Nakahara and Hikita [9] have also observed melting during ignition. They measured a maximum combustion temperature of 1500°C for a 60% $Sb/KMnO_4$ mixture. At such temperatures even gas-phase oxidation of antimony vapour could be involved.

Reaction intermediate and products

At high percentage fuel, the only species identifiable by XRD in the ignition product, were Mn_3O_4 and residual Sb metal. At lower percentage fuel ($\leqslant 30\%$), possible products were $K_2Mn_4O_8$, Mn_2O_3, α-Mn and $KMnO_2$. No crystalline compounds of antimony were identified, and it is possible that any such compounds may be present as inorganic glasses, amorphous to X-rays [16].

IR spectra (in KBr) gave some additional information. The main absorption peaks [17,18] for $KMnO_4$ (Fig. 10a) are at 895 cm^{-1} (with a shoulder at ~ 920 cm^{-1} and a sharp but weaker peak at 838 cm^{-1}) and a doublet at 396 and 380 cm^{-1}. The peak at 895 cm^{-1} is still evident in the spectra of the products of the first and second stages of the $KMnO_4$ decomposition (Fig. 10b and c, respectively), although it is reduced in size. K_2MnO_4 is proposed [5] as being one of the solid products of the first stage of the decomposition of $KMnO_4$, and the IR spectrum of a sample of K_2MnO_4, prepared from solution, is shown in Fig. 11a. The main absorption is at ~ 835 cm^{-1}. The absorption at ~ 895 cm^{-1} is probably due to residual MnO_4^-. The spectrum of the product of decomposition of K_2MnO_4 in air is shown in Fig. 11b.

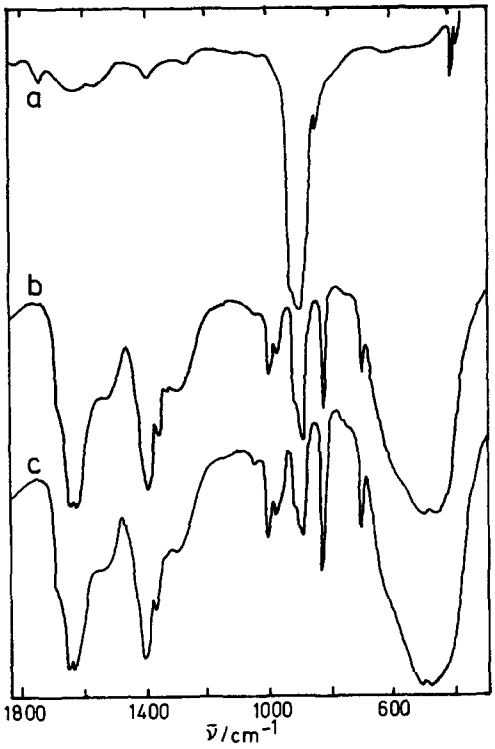

Fig. 10. IR spectra of (a) $KMnO_4$; (b) product of first stage of $KMnO_4$ decomposition in air; and (c) product of the second stage of the $KMnO_4$ decomposition in air.

Peaks have developed not only in the metal–oxygen region (400–700 cm^{-1}), but also in the 1300–1700 cm^{-1} region and the peak at 835 cm^{-1}, associated with MnO_4^{2-}, is still strong. The spectrum of the product of the K_2MnO_4

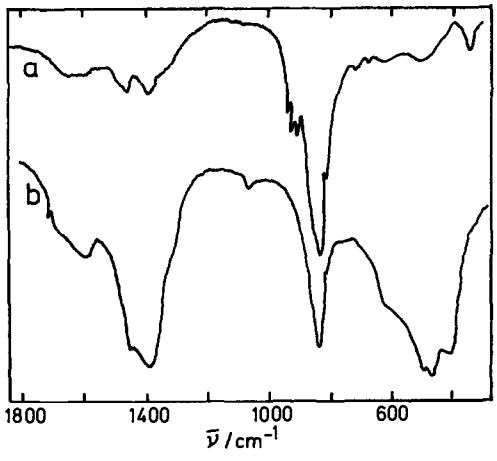

Fig. 11. IR spectra of (a) K_2MnO_4; (b) product of the K_2MnO_4 decomposition in air.

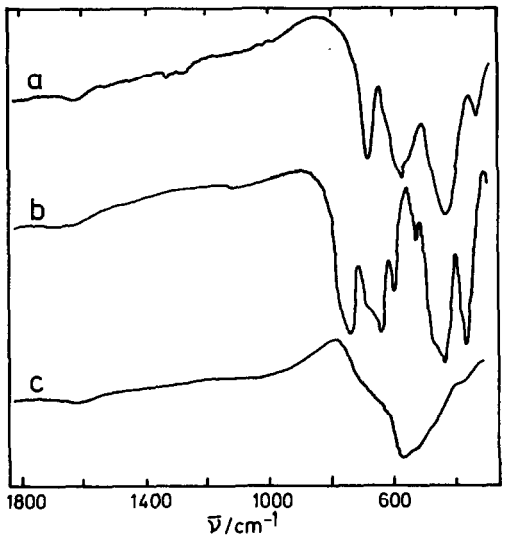

Fig. 12. IR spectra of (a) Sb_2O_3; (b) Sb_2O_4; (c) MnO_2.

decomposition (Fig. 11b) differs considerably from that of the final product of the $KMnO_4$ decomposition (Fig. 10c). The other solid product of the $KMnO_4$ decomposition, labelled as $K_4Mn_7O_{16}$, is reported [5] to interact strongly with water and carbon dioxide from the atmosphere. This is evident in the IR spectra (Fig. 10b and c) with strong peaks at 1630 cm^{-1} and 1400 cm^{-1} due to HCO_3^- [19]. Water also absorbs around 1600 cm^{-1}. The spectrum of $KHCO_3$ (ref. 17, spectrum 55) has strong absorptions at 1650,

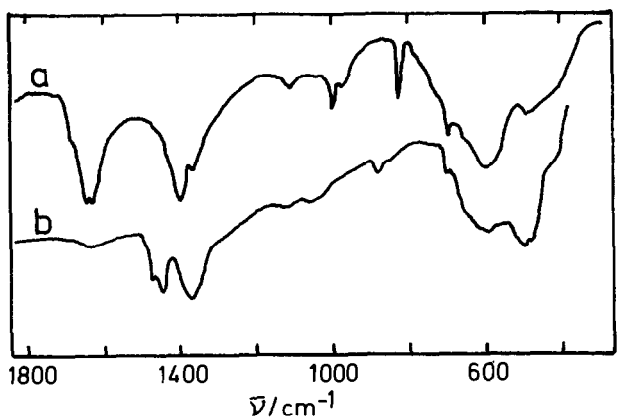

Fig. 13. IR spectra of (a) the product of ignition of 60% $Sb/KMnO_4$ in air; (b) the product of heating 60% $Sb/KMnO_4$ in nitrogen to 720°C without ignition.

1400, 1000, 835 and 700 cm^{-1} which are all apparent in Fig. 10b and c. The product of the K_2MnO_4 decomposition (Fig. 11b) seems to contain CO_3^{2-} rather than HCO_3^- [17]. This may depend on the availability of H_2O, which was not controlled. These secondary reactions complicate the interpretation of the IR spectra and would tend to mask the presence of intermediate K_2MnO_4, since there are strong carbonate and MnO_4^{2-} absorptions around 835 cm^{-1}. The less-affected metal–oxygen region (< 700 cm^{-1}) shows the development of strong but broad absorptions (Figs. 10 and 11). The spectrum of MnO_2 is shown in Fig. 12c for comparison.

IR spectra of the product of ignition of a sample of a 60% Sb/$KMnO_4$ mix in a delay element, and of the product of another sample heated in nitrogen to 720°C without ignition are shown in Fig. 13a and b, respectively. These spectra indicate that there are considerable differences in the products formed when an 'external' supply of oxygen is available and when it is absent. The spectrum of the product of ignition (Fig. 13a) resembles those of the products of $KMnO_4$ decomposition (Fig. 10b and c) including interaction with CO_2 and H_2O, with the main differences being the total absence of the peak at 895 cm^{-1}, attributed to residual permanganate, and the modifications to the broad band in the 300–800 cm^{-1} region, probably through contributions from the Sb–O system. (The spectra of Sb_2O_3 and Sb_2O_4 are given in Fig. 12a and b). The complete absence of MnO_4^- ions may be a result of the higher temperatures reached during ignition or some interaction or catalytic effect [20] of antimony compounds, or both.

Changes in fuel or oxidant

When $KMnO_4$ in the pyrotechnic compositions is replaced by $RbMnO_4$, the reactions, as expected, appear to be little altered.

The results obtained for the effect of the presence of Mn on the oxidation of Sb suggested that a similar effect might be operating in the Sb/$KMnO_4$ system. Mn powder has been successfully used as a fuel with $KMnO_4$ in pyrotechnic compositions [20] but the ignition reaction does not occur below the 720°C limit of the DSC. When MnSb was used as a fuel with $KMnO_4$, the DSC trace (Fig. 14a) had two exotherms, a broad one at ~ 500°C and a sharper one at ~ 580°C, which is the temperature at which MnSb oxidises in air (Fig. 14b). Another relevant trace is that for the reaction of a 50% Sb/MnO_2 mixture in air (Fig. 14c), where a strongly exothermic reaction occurs just above 500°C. MnO_2, on heating by itself in air [21], immediately begins to decompose slowly and endothermally, accelerating around 500°C to a maximum at about 580°C. Oxygen is thus being produced at temperatures very close to the ideal temperature range for the oxidation of Sb. The endothermic effect of the MnO_2 decomposition may, however, counteract the exothermic oxidation of Sb to some extent and hence not lead to an ideally sharp ignition exotherm.

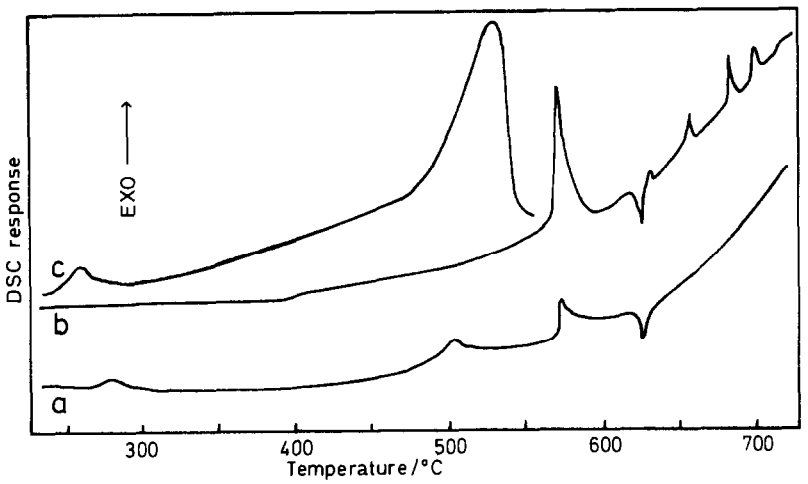

Fig. 14. DSC on (a) 50% $MnSb/KMnO_4$; (b) MnSb; (c) 50% Sb/MnO_2 in air at 20°C min^{-1}.

CONCLUSIONS

Samples of $Sb/KMnO_4$ compositions can be made to undergo ignition during thermal analysis, provided that the sample mass and the heating rate are not too low, and that oxygen is available in the carrier gas. In sealed delay elements the oxygen required is supplied by the first stage of the thermal decomposition of the $KMnO_4$. One of the solid products of this decomposition stage is proposed to be K_2MnO_4. Mixes of Sb with K_2MnO_4 synthesised from solution, as well as mixes of Sb with partially decomposed $KMnO_4$, ignite on heating in air, but do not fire in delay elements. Heating $Sb/KMnO_4$ mixtures in flowing nitrogen, which flushes the initially evolved oxygen from the system before the main reaction temperatures are reached, results in a more diffuse exothermic interaction without change in mass. The product, on reheating in air, oxidises more slowly and less completely without showing an ignition exotherm.

Antimony, heated on its own in air, undergoes some surface oxidation at ~ 300°C and then oxidises in several stages between 300 and 600°C, giving Sb_2O_4 as the final product, with simultaneous volatilisation of some Sb_2O_3. The course of the oxidation is influenced by the presence of Mn (Fig. 4) either in a physical mixture, or as the intermetallic compound MnSb.

The temperature range (480–520°C) over which the ignition process in $Sb/KMnO_4$ mixes occurs, corresponds to the temperatures at which the formation of Sb_2O_3 is rapid during the oxidation of Sb in air (Fig. 3). The presence of the solid residue from the first stage of the decomposition of $KMnO_4$, or from the decomposition of K_2MnO_4 prepared from solution, or MnO_2, or Mn (as a mixture or as the intermetallic compound, MnSb) all influence the oxidation of Sb by gaseous oxygen. In $Sb/KMnO_4$ mixes with

high percentages of Sb, two partially-concurrent oxidations seem to occur: Sb in a straight solid–gas reaction, and an overall solid–solid–gas reaction involving Mn in an undetermined form. One of the effects, of all but the metal itself, could be the supply of oxygen by further decomposition of oxides (of varying complexity) catalysed by Sb or Sb oxides. There is no evidence for formation amongst the ignition products, of crystalline compounds of Sb. There is thus the possibility of formation of glasses containing K, Mn, Sb and oxygen.

ACKNOWLEDGEMENTS

The support of AECI Ltd. and of the South African CSIR are gratefully acknowledged, as are helpful discussions with Mr. C.W. Ehmke, Dr. D. Cawthorne, Miss M. Le Patourel, Miss A. Head and Dr. V. Joynt. Miss M. Mayer supplied the X-ray diffraction data.

REFERENCES

1 E.L. Charsley, C.T. Cox, M.R. Ottaway, T.J. Barton and J.M. Jenkins, Thermochim. Acta, 52 (1982) 321.
2 A.J. Beardell, J. Staley and C. Campbell, Thermochim. Acta, 14 (1976) 169.
3 A.J. Beardell and A.D. Kirshenbaum, Thermochim. Acta, 8 (1974) 35.
4 T. Boddington, P.G. Laye, J.R.G. Pude and J. Tipping, Combust. Flame, 47 (1982) 235.
5 F.H. Herbstein, G. Ron and A. Weissman, J. Chem. Soc. A, (1971) 1821; Proc. 3rd Int. Conf. Therm. Anal., Vol. 2, 1971, p. 281; J. Chem. Soc. Dalton, Trans., (1973) 1701.
6 J.S. Booth, D. Dollimore and G.R. Heal, Thermochim. Acta, 39 (1980) 281, 292.
7 S.E. Golunski, T.G. Nevell and M.I. Pope, Thermochim. Acta, 51 (1981) 153.
8 S. Nakahara, J. Ind. Exp. Soc., Jpn., 22 (1961) 259.
9 S. Nakahara and T. Hikita, Kogyo Kayaku Kyokai-Shi, 20 (1959) 356; 21 (1960) 2.
10 T. Gymkowski, D.G. Lambert and H.S. Kimmel, J. Inorg. Nucl. Chem., 34 (1972) 1841.
11 R. Scholder and H. Waterstradt, Z. Anorg. Chem., 277 (1954) 172, 234.
12 P.J. Herley and E.G. Prout, J. Phys. Chem., 64 (1960) 675.
13 V.V. Boldyrev, Z.G. Vinokurova, L.N. Senchenko, G.P. Shchetinina and B.G. Erenburg, Russ. J. Inorg. Chem., 15 (1970) 1341.
14 V.V. Boldyrev, A.P. Vorinin, T.A. Nevolina and V.V. Morusin, J. Solid State Chem., 20 (1977) 327.
15 F.D. Rossini, D.D. Wagman, W.H. Evans, S. Levine and I. Jaffee, Selected Values of Chemical Thermodynamic Properties, Natl. Bur. Stand., U.S., Circ. 500, Washington, 1952.
16 P.J. Miller and C.A. Cody, Spectrochim. Acta Part A, 38 (1982) 555.
17 R.A. Nyquist and R.O. Kagel, Infrared Spectra of Inorganic Compounds, Academic Press, New York, 1971.
18 P.J. Hendra, Spectrochim. Acta Part A, 24 (1968) 125.
19 P.M. Maguire and H.E. Rubalcava, Inorg. Chem., 8 (1969) 246.
20 J.E. Spice and L.A.K. Staveley, J. Soc. Chem. Ind., 68 (1949) 348.
21 T. Ohzuku, I. Tari and T. Hirai, Electrochim. Acta, 27 (1982) 1049.